Measurement of Cosmic Deuteron Flux with the AMS-02 Detector

Measurement of Cosmic Deuteron Flux with the AMS-02 Detector

F Dimiccoli[1], R Battiston[1], K Kanishchev[1], F Nozzoli[1] and P Zuccon[1,2]

[1] INFN, Trento Institute for Fundamental Physics and Applications, I-38123, Trento, Italy
[2] Università degli Studi di Trento, I-38123 Trento, Italy

E-mail: francesco.dimiccoli@unitn.it

Abstract. The deuteron flux in cosmic rays is one of the most valuable tools for understanding the propagation of CR in the galaxy and constrain the models that describe it. In this work, a new preliminary measurement of D flux is presented, obtained from the data of the AMS-02 experiment.

1. Introduction

The importance of the measurement of light isotopic components in cosmic rays (CR) like deuterons (D) resides in their production by spallation reactions of primary CR protons and ^{4}He nuclei on the protons of the Inter Stellar Medium (ISM). The measurement of these components with respect to their respective primary can provide important constrains about the CR residence time within galaxy and their propagation history. [1,2]. In general, light isotopes originate from the spallation of heavier ones, for example D from ^{3}He and ^{4}He. Another source of deuterons in CR is the p-p fusion in the CR collision with the ISM at extremely low energies (below 1 GeV/n). Their abundance, provide additional and complementary information with respect to the most common tool used for propagation studies, the Boron over Carbon (B/C) flux ratio. Due to the smaller interaction cross sections D can probe the propagation distance parameter in an energy range useful for better constraining the anti-proton background for cosmic antimatter searches [3]. Furthermore, the low energy threshold of the p-p fusion reaction makes the D/p ratio measurement useful to constrain propagation models at very low energies.

2. The Instrument: AMS-02

The Alpha Magnetic Spectrometer (AMS-02) [4–19] is a particle detector installed on International Space Station, whose components include a solid state tracker for determination of charge and rigidity, defined as $R = p/Z$ (where p is the particle momentum), a Time of Flight detector (ToF) and a Cherenkov detector (RICH) for particle velocity measurement, a Transition Radiation Detector (TRD) and an Electromagnetic CALorimeter (ECAL) for hadron/lepton discrimination. The Tracker is composed by 7 layers inside the magnetic volume (inner Tracker), plus two external layers, one above the TRD and one above the ECAL (respectively, L1 and L9). A scheme of the AMS-02 detector is presented in Fig. 1, with all the main subdetectors highlighted.

Thanks to its wide acceptance and privileged position above the Earth's atmosphere, AMS-02 has been providing compelling science, having collected more than 150 billions of charged CR since 2011. Data from published AMS-02 results are online in the ASI/SSDC database [20].

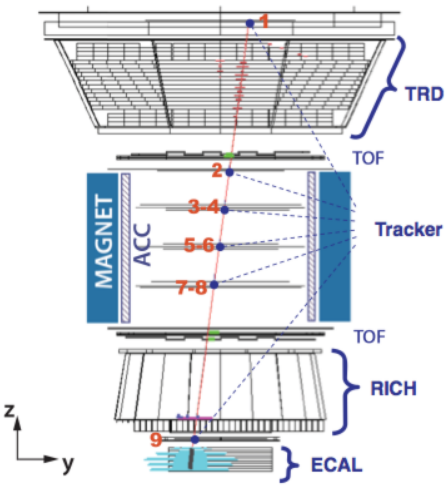

Figure 1. Scheme of the AMS-02 detector. From the top, tracker first layer (1), TRD, upper ToF, inner tracker layers (2,3,4,5,6,7,8), lower ToF, RICH, tracker layer 9 and ECAL. Sixteen curved scintillator panels (Anti-Coincidence Counters, ACC) surround the inner tracker inside the 0.14T magnet bore.

3. Isotope identification with AMS-02

The identification of D from the proton dominant components is performed in AMS-02 with the concurrent measurement of Rigidity and velocity ($\beta = v/c$), which provide a mass measurement:

$$m = ZR/\gamma\beta \; . \tag{1}$$

This mass identification is performed starting from a $Z = 1$ sample, obtained with charge measurement at different levels within the detector. Additional selections have been implemented to reject most of events suffering from interactions within the detector. The rigidity is measured by the inner Tracker, while the velocity by ToF and RICH. The β resolution of ToF ($\sim 2\%$) allows isotopic distinction up to 0.85 GeV/n. At higher energies, AMS-02 RICH is used. This detector is equipped with two different radiators, Sodium Fluoride (NaF) and Aerogel (Agl), with different values of thresholds and resolutions, allowing isotopic distinction in the Kinetic energy per nucleon range from 0.7 to 3.2 GeV/n (NaF) and from 2.7 to 8.9 GeV/n (Agl). In the combined range 0.2-8.9 GeV/n, the rigidity measurement has a resolution of 8%, which dominates the overall mass resolution. Such limited resolutions prevent the event-by-event identification of isotopes and makes a template fit approach, on the reconstructed mass distribution, necessary for both analyses. In general, the separation is performed dividing each range in narrow bins of measured β, to exploit the higher precision of the velocity measurement and minimize bin migration effects. The result is

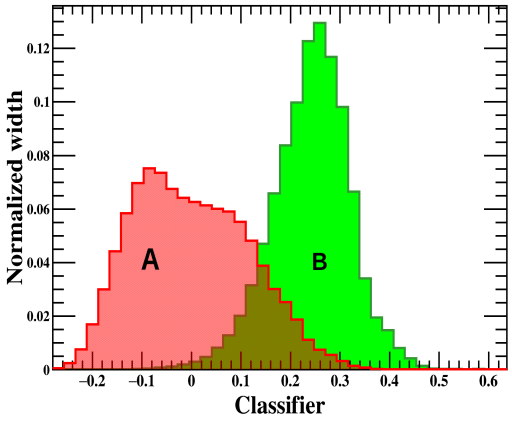

Figure 2. Distribution of RICH BDT classifier on background (A) and signal (B).

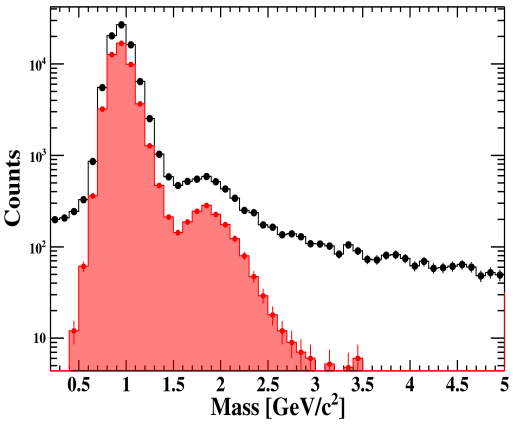

Figure 3. Mass distribution in a particular velocity bin of RICH velocity before (black dots) and after (red distribution) RICH BDT cut.

given in terms of rigidity on top of the instrument (T.o.I.) i.e. considering the particle energy loss that is not negligible in the low beta region.

3.1. Deuteron mass distribution

The templates have been obtained from Monte Carlo (MC) simulations. The detector resolutions in MC has been optimized according to flight data as explained in the following section, to provide matching with the data mass distributions. For the measurement in the ToF energy range, dedicated selections on the time of flight measurement, such as selections on the temporal and spatial consistency of the clusters, were optimized to reduce the background of mis-reconstructed particles. A geometrical matching was also required between the clusters in the ToF paddles and the track measured by the inner tracker.
In the RICH energy regions, a more elaborate technique is needed to reject a particular source of background, described below. The number of photons produced by Cherenkov effect is proportional to Z^2, therefore only 3-4 photons are collected by RICH for charge-one particles. This makes the measurement of velocity for such particles particularly challenging for this instrument. It is possible, in fact, that a spurious hit spoils the ring fit procedure and produce a wrong velocity measurement. Such background was characterized and turned out to be caused by extra hits mostly coming from back-splash electrons from ECAL, which tipically cause a lower velocity reconstruction of fast particles. This effect is responsible for an high mass proton tail overlapping the deuteron signal. A multivariate (BDT - Boosted Decision Trees) classifier was trained on a set of variables sensible to this effect, in particular the number of hits ignored by the ring fit and the ratio between the number of expected and measured photo-electrons for a charge-one particles. The training samples were selected directly from flight data, using the following criteria:

- *Background:* mass > 3.5 (no stable Z=1 particle is expected for A> 2)
- *Signal:* $0.5 <$ mass < 1.5 (the bulk of proton signal)

A cut in the resulting classifier (Fig. 2) is able to increase the signal to noise ratio by more than one order of magnitude (Fig. 3).

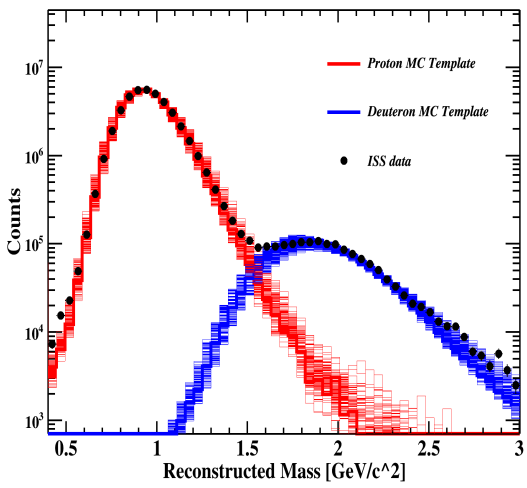

Figure 4. Example of multiple fit performed in a particular bin of ToF region considering the systematic uncertainties in the template definition.

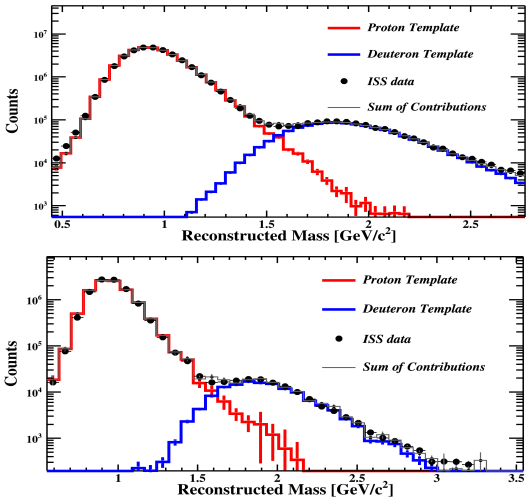

Figure 5. Example of template fits of mass distributions in a particular bin of ToF (above) and RICH (below) energy regions.

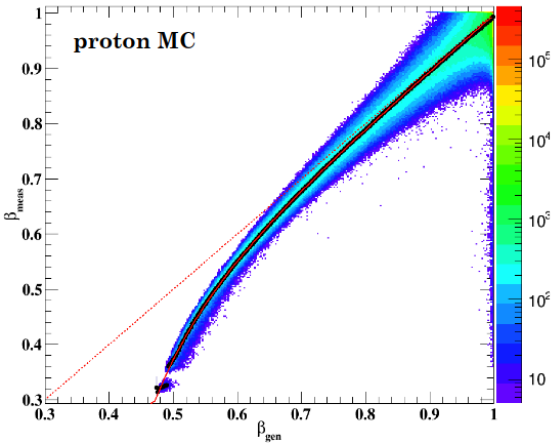

Figure 6. Effect of energy loss on reconstructed velocity of MC generated protons. The relation between measured β vs $\beta_{T.o.I.}$ was modeled in MC (red curve) and used for the energy loss correction as described in the text.

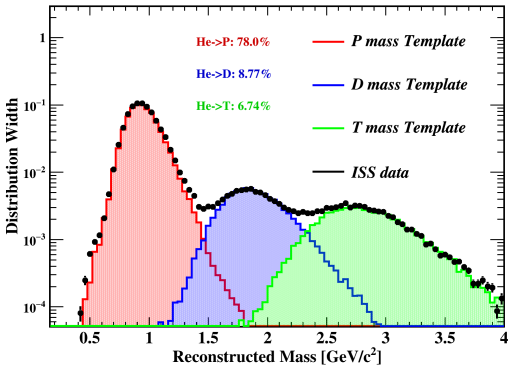

Figure 7. Example of the mass distribution of He fragments, obtained after the subtraction procedure described in the text. The distribution is fitted with three contributions: p, D and T. At low reconstructed mass the presence of secondary produced mesons in the He fragmentation process is visible.

3.2. Deuteron identification

The deuteron separation from proton background is performed using a template fit technique on the mass distributions. The templates for proton and deuteron components were obtained by MC simulation data-sets undergoing the same selections applied on data. Moreover, the detector resolution simulated in the MC was fine-tuned to match the flight data. In particular, for the sub-detectors:

- *ToF:* tuning the time resolution.
- *RICH:* tuning the measured Cherenkov angle.

To evaluate the systematic uncertainty in the result due to the template definiton, a marginalization over the sub-detector resolution parameters was performed considering (~ 100) different configurations weighted by the parameter's likelihood probability (see Fig. 4). Figure 5 shows two examples of the fit performed respectively in the ToF and RICH energy regions.

3.3. Evaluation of energy loss effect

To obtain the D flux in cosmic rays, a correction for energy loss effects within the detector is necessary. The energy loss is caused by ionization within in the detector before the inner tracker, mostly in TRD and ToF, and being $\propto 1/\beta^2$, the fraction of this energy loss over the total is very different for different isotopes. This results in a different migration of proton and deuteron events toward lower velocity, and prevents the use of a common measured beta regions to evaluate proton and deuteron flux as a function of $\beta_{T.o.I.}$. This energy loss was modeled using MC simulations (Fig. 6) with the parametrization:

$$\Delta\beta = \frac{1}{m}\frac{\alpha}{\beta^{\gamma}} \ , \tag{2}$$

where $\alpha \simeq 0.0035$ and $\gamma \simeq 5.84$ are the parameters of the model. The effect of energy loss is accounted for each $R_{T.o.I.}$ and for a fixed particle, i.e. the $R_{T.o.I.}$ interval is converted in $\beta_{T.o.I.}$ using the (1) and converted to a measured β interval with (2). An independent mass fit is performed for every measured velocity bin for each isotope, using the methods described above.

3.4. Evaluation of fragmentation effect

The fragmentation regards the production of secondary nuclei of p, D and T from the fragmentation of primary ^{3}He or ^{4}He, mostly due to interactions in the material of AMS-02. The background coming from this effect can be divided into two categories:

- Fragmentation *below* layer 1 of the tracker: mostly in TRD and upper paddles of ToF.
- Fragmentation in the very small amount of material *above* layer 1.

The first source of background is effectively reduced to a negligible level requiring an hit in layer 1 of tracker matching the track reconstructed by the inner tracker. The second one is not reducible and needs to be evaluated to avoid biases in the final flux. To minimize systematic effects in the MC description of He fragmentation processes, a pure data-driven methodology has been developed. Exploiting the full statistics provided by AMS-02 is possible to spot a relatively small contribution of T in the data mass distribution of cosmic charge-one particles. Since T is a relatively fast decaying isotope ($T_{1/2} = 12.3$ y), it is believed to be substantially absent in *galactic* cosmic rays, and thus is mostly produced by the above mentioned interactions. For this reason, its amount can be used as a measurement of the rate of He fragmentation processes. To measure the quantity of secondary D background, however, also a measurement of the branching ratio of the fragmentation reaction is needed. An estimation of fragmenting He mass distribution was obtained selecting a sample of charge-two particles on top of the instrument (tracker layer 1) and selecting events whose charge measured by the inner tracker is compatible with one. This sample is contaminated by a residual tail of galactic protons/deuterons surviving to the tracker layer 1 charge-two selection cut. This contribution was evaluated by a template fit of the unselected charge distribution of tracker layer 1 and subtracted to obtain an unbiased mass distribution of the fragments. Figure 7 shows an example of the mass distribution of He fragments obtained with this method, with the three contributions (p, D and T) separated. Such mass distribution can be fitted using the same techniques discussed in section 3.2, to obtain a measurement of T/D ratio coming from fragmentation. A ratio of ~ 0.9 was measured throughout the full energy range of the analysis, resulting in a contamination of $\sim 2\%$ of the deuteron signal given by deuterons from He fragmentation. The result of this data-driven fragmentation measurement is stable within a 10% level using a different level of selections on the charge reconstructed by the

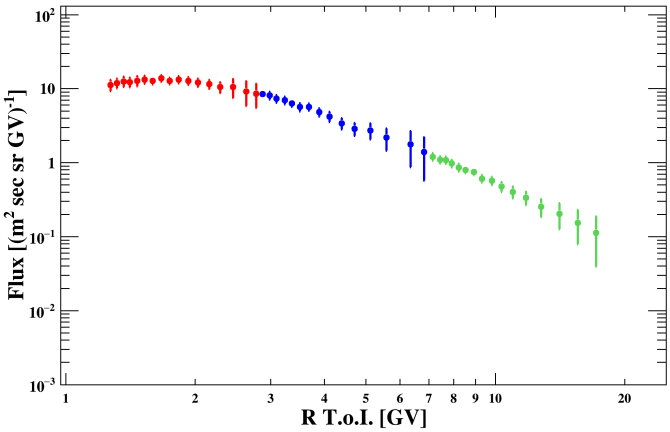

Figure 8. Preliminary: measurement of D flux measured by the AMS-02 experiment, obtained with ToF (red), RICH NaF (blue) and Agl (green). The uncertainties include preliminary (cautious) evaluation of systematic error.

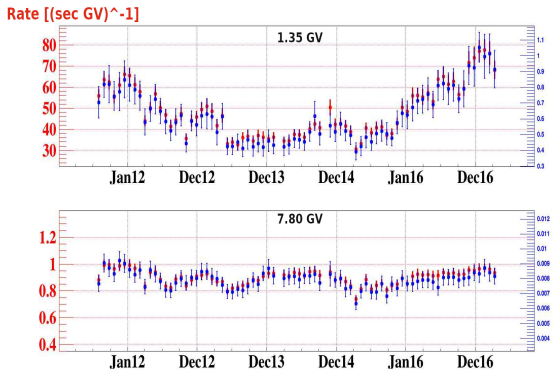

Figure 9. Preliminary: time dependence of the D rate (blue) compared with the P one (red) in two different rigidity bins.

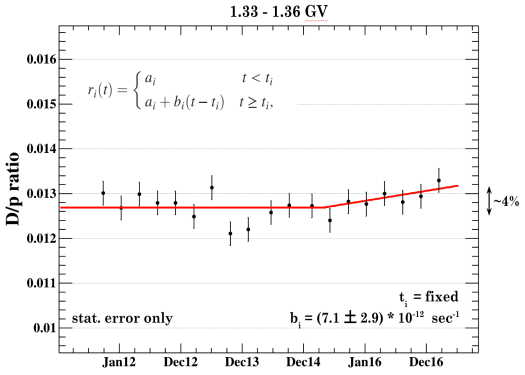

Figure 10. Preliminary: time dependence of the D/p rate ratio in the 1.33-1.36 GV rigidity range. In the fit, t_i was fixed to the February 28, 2015 value [16].

layer 1 of the tracker for the initial He sample.

4. Conclusions

The D flux in CR measured by the AMS-02 experiment extends in energy regions substantially uncharted by the previous measurements over a total period of 7 yrs all over the 24^{th} solar cicle, and present an accuracy of the order of few percent (Fig. 8). The high acceptance of the instrument allowed to measure the time dependece of the p and D fluxes at different rigidities (Fig. 9), using time bins corresponding to one single Bartel rotation ($\sim$ 28 days). In general, the overall cosmic ray flux is *anti-correlated* with solar activity. On top of this general behaviour, the D flux shows the same time structures of the proton one. In particular, first hints of a small time dependence of the D/p flux ratio were found in the extremely low rigidity bins. Such time dependence is shown in Fig. 10 and modeled with the relation reported in the same figure. Its maximum amplitude in the period analyzed is $\sim 4\%$.

References

[1] Coste B *et al.* 2012 *Astron. Astrophys.* **539**
[2] Tomassetti N, Feng J 2017 *Astrophys. J. Lett.* **835**
[3] Gomez-Coral D *et al.* 2018 *Phys. Rev. D* **98** 023012
[4] *AMS Official website* https://ams02.space/
[5] Aguilar M *et al.* 2013 *Phys. Rev. Lett.* **110** 141102
[6] Accardo M *et al.* 2014 *Phys. Rev. Lett.* **113** 121101
[7] Aguilar M *et al.* 2014 *Phys. Rev. Lett.* **113** 121102
[8] Aguilar M *et al.* 2014 *Phys. Rev. Lett.* **113** 221102
[9] Aguilar M *et al.* 2015 *Phys. Rev. Lett.* **114** 171103
[10] Aguilar M *et al.* 2015 *Phys. Rev. Lett.* **115** 211101
[11] Aguilar M *et al.* 2016 *Phys. Rev. Lett.* **117** 091103
[12] Aguilar M *et al.* 2016 *Phys. Rev. Lett.* **117** 231102
[13] Aguilar M *et al.* 2017 *Phys. Rev. Lett.* **119** 251101
[14] Aguilar M *et al.* 2018 *Phys. Rev. Lett.* **120** 021101
[15] Aguilar M *et al.* 2018 *Phys. Rev. Lett.* **121** 051103
[16] Aguilar M *et al.* 2018 *Phys. Rev. Lett.* **121** 051101
[17] Aguilar M *et al.* 2018 *Phys. Rev. Lett.* **121** 051102
[18] Aguilar M *et al.* 2019 *Phys. Rev. Lett.* **122** 041102
[19] Aguilar M *et al.* 2019 *Phys. Rev. Lett.* **122** 101101
[20] *ASI/SSDC cosmic ray database* https://tools.ssdc.asi.it/CosmicRays/